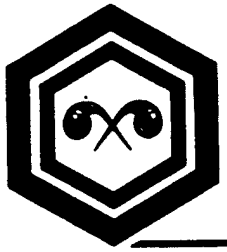

EDGEWOOD
RESEARCH, DEVELOPMENT & ENGINEERING CENTER
U.S. ARMY CHEMICAL AND BIOLOGICAL DEFENSE COMMAND

ERDEC-TR-273

EQUILIBRIUM-VAPOR CELL FOR QUANTITATIVE INFRARED ABSORBANCE MEASUREMENTS

P.E. Field

VIRGINIA POLYTECHNIC INSTITUTE AND STATE UNIVERSITY
Blacksburg, VA 24061-0212

R.J. Combs
R.B. Knapp

RESEARCH AND TECHNOLOGY DIRECTORATE

August 1995

Aberdeen Proving Ground, MD 21010-5423

Disclaimer

The findings in this report are not to be construed as an official Department of the Army position unless so designated by other authorizing documents.

REPORT DOCUMENTATION PAGE

Form Approved
OMB No. 0704-0188

1. AGENCY USE ONLY *(Leave blank)*	2. REPORT DATE	3. REPORT TYPE AND DATES COVERED
	1995 August	Final, 93 Jul - 94 Feb

4. TITLE AND SUBTITLE
Equilibrium-Vapor Cell for Quantitative Infrared Absorbance Measurements

5. FUNDING NUMBERS
PR-56553J8D13
C-DAAD05-93-W-0997

6. AUTHOR(S)
Field, P.E. (VPI&SU), Combs, R.J., and Knapp, R.B. (ERDEC)

7. PERFORMING ORGANIZATION NAME(S) AND ADDRESS(ES)
Virginia Polytechnic Institute and State University,
Blacksburg, VA 24061-0212
DIR, ERDEC, ATTN: SCBRD-RT, APG, MD 21010-5423

8. PERFORMING ORGANIZATION REPORT NUMBER
ERDEC-TR-273

9. SPONSORING / MONITORING AGENCY NAME(S) AND ADDRESS(ES)

10. SPONSORING / MONITORING AGENCY REPORT NUMBER

11. SUPPLEMENTARY NOTES

12a. DISTRIBUTION / AVAILABILITY STATEMENT
Approved for public release; distribution is unlimited.

12b. DISTRIBUTION CODE

13. ABSTRACT *(Maximum 200 words)*

Infrared (IR) absorbance measurements, through a gas flow cell, are made with the closed-loop circulation of vapor-air mixtures that are generated by temperature equilibrated aqueous solutions. Accurate vapor pressures of organic solutes are established with the equilibrated aqueous solutions. The water solvent effectively depresses the vapor pressure associated with the pure organic solutes of methanol, ethanol, isopropanol, acetone, and methyl ethyl ketone (MEK). Knowledge of the solute liquid mole fractions, pure component vapor pressures, and the Wilson equation permit determination of the solute vapor pressures to within 2% accuracy. Reliable solution preparation requires only the correct weighings of pure constituent materials before mixing to achieve the targeted solute liquid mole fractions. Absorbances are measured for all solutes over a range of seven concentrations with the exception of four MEK concentrations. These concentrations show the absorbance region of adherence to Beer's Law with an experimental precision of approximately ±2% for the solutes studied. Absorptivities that are calculated from the absorbance versus vapor pressure slopes are compared to the available IR absorbance data from other laboratories.

14. SUBJECT TERMS
Vapor pressure
IR absorptivity
Fourier transform spectrometry

15. NUMBER OF PAGES
28

16. PRICE CODE

17. SECURITY CLASSIFICATION OF REPORT	18. SECURITY CLASSIFICATION OF THIS PAGE	19. SECURITY CLASSIFICATION OF ABSTRACT	20. LIMITATION OF ABSTRACT
UNCLASSIFIED	UNCLASSIFIED	UNCLASSIFIED	UL

Blank

PREFACE

The work described in this report was authorized under Project No. 56553J8D13 and Contract No. DAAD05-93-W-0997. This work was started in July 1993 and completed in February 1994.

The use of trade or manufacturers' names in this report does not constitute an official endorsement of any commercial products. This report may not be cited for purposes of advertisement.

This report has been approved for public release. Registered users should request additional copies from the Defense Technical Information Center; unregistered users should direct such requests to the National Technical Information Service.

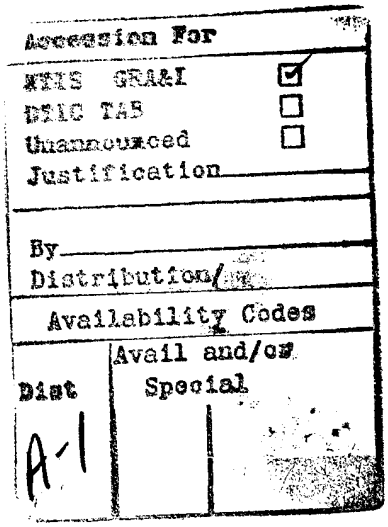

Blank

CONTENTS

FIGURES

TABLES

EQUILIBRIUM-VAPOR CELL FOR QUANTITATIVE INFRARED ABSORBANCE MEASUREMENTS

1. INTRODUCTION

The detection and quantification of volatile organic compounds (VOCs) at hazardous waste sites are important in determining the necessary steps for remediation. Open-path Fourier transform infrared (FTIR) spectrometry provides an effective method of monitoring for these VOCs.[1,2] A variety of approaches for detection of VOCs with open-path FTIR spectrometry are documented.[3-6]

This investigation furnishes a vapor-cell method for generation of known vapor concentrations. This vapor-cell approach differs from the traditional methods of vapor generation for static gas cell measurements.[7,8] The equilibrium-vapor cell (EVC) relies on the maintenance of a constant vapor concentration by establishment of equilibrium with the continuous circulation of an air-vapor mixture through a fixed composition aqueous solution. Aqueous solutions are used for convenience. These solutions also permit a reliable assessment of water vapor concentration, as well as VOC solute vapor pressure. Aqueous solutions necessitate that the VOC be completely miscible. Binary aqueous solutions of methanol, ethanol, isopropanol, acetone, and methyl ethyl ketone (MEK) are used.

Experimental determination of the vapor concentrations of non-ideal aqueous solutions is extremely difficult. The EVC method relies on the accurate weighing in solution preparation and on the proper temperature equilibration in using the prepared aqueous solution. Inputs of liquid composition and solution temperature permit determination of the vapor concentration for the solute and solvent with the Wilson equation.[9] The Wilson equation is accurate to within 2% for the systems studied. This requires a realistic assessment of the Wilson coefficients from the available literature vapor data.[10] The EVC absorbance measurements are made with a conventional MIDAC (Irvine, CA) FTIR spectrometer. The absorbance measurements are shown adherence to Beer's Law over a range of vapor pressures. The slope of the absorbance versus the vapor concentration is the absorptivity-pathlength product. The absorptivity is obtained by dividing this product with the cell pathlength. The experimentally determined absorptivity is compared with those from other laboratories for five solute vapors.

2. EXPERIMENTAL METHODS

The FTIR spectrometer is equipped with a liquid nitrogen cooled Hg:Cd:Te detector (model no. HCT-21A,

serial no. P-14319, Infrared Associates, Incorporated, Cranbury, NJ). The laboratory spectrometer is a MIDAC, model 101280 (serial no. 106, MIDAC Corporation, Irvine, CA). The laboratory spectrometer detector has a spectral range of 400 to 4000 cm^{-1}.

Interferogram data was collected with Spectra Calc at 2 cm^{-1} spectral resolution for all vapors generated with aqueous solutions, as well as 0.56 cm^{-1} resolution for only the methanol vapor.[11] Interferograms of 100 coadditions were collected with the laboratory spectrometer. Analysis of the interferogram and spectral data was performed in Spectra Calc.

The equilibrium-vapor cell consists of readily available components. Figure 1 is a schematic of the equilibrium-vapor cell. The circulating pump model 81-012 (Universal Electric Company, Owosso, MI), demountable 10-cm gas cell, model 7200 (Buck Scientific, East Norwalk, CT) with zinc selenide windows, and bubbler are interconnected with tygon tubing. The bubbler, which contains 125 mL aqueous solution, is immersed in a constant temperature bath model RTE-111 (Neslab Instruments Incorporated, Newington, NH). The recycling of the air-vapor mixture through the aqueous solution achieves equilibrium in the gas cell after approximately 10 min. The bath is set at a temperature of 22 °C, which is below the ambient room temperature. This avoids condensation of vapors in the connection tubes, pump, or demountable cell. The bath temperature is monitored with a calibrated negative temperature coefficient thermistor.

Aqueous solutions were prepared by weight percent. Weights of solution components were made on a model AE200 top loading balance (Mettler Instruments Corporation, Hightstown, NJ). Distilled/deionized water was used in solution preparation. The sequence of solutions used in the absorbance measurements proceeded from most dilute to most concentrated. This avoided any potential problems with vapor absorption/desorption in the equilibrium-vapor cell apparatus.

3. RESULTS AND DISCUSSION

The dependence of the IR absorbance on the partial vapor pressure of five organic solvents is examined for methanol, ethanol, isopropanol, acetone, and MEK. The partial vapor pressures for all but three measurements range from 5 to 50 millibars at 22 °C. Various concentrations of binary aqueous solutions provide seven evenly distributed vapor pressures. The liquid mole fractions and vapor pressures at 22 °C of the binary solutions are tabulated in Table 1.

Accurate determination of the vapor pressure is essential to the quantitative evaluation of the IR absorbances.

All of the binary solutions considered in this study exhibit non-ideal solution behavior. Therefore, the empirical evaluation of the activity coefficients of the solution components becomes necessary to account for the excess solution free energy of mixing. Rather than rely on a single data set, the approach of this investigation follows a modified version of Hirata et al.[10] to obtain the best pair of Wilson coefficients for each binary solution. Based on the analysis of the various empirical methods for evaluation of the activity coefficients, Hirata et al. maintained that Wilson's equation is the most reliable for a broad range of systems including those in this study.

The Wilson equation accounts for the excess solution free energy of mixing by extending the Flory and Huggin's theoretical equation for athermal solutions.[9] The relative probabilities of dissimilar neighboring molecules, within a local volume fraction, permits derivation of the Wilson coefficients. These coefficients, along with solution mole fractions, allow a determination of the excess free energy of mixing. The Wilson equation for determining the activity coefficient is subsequently derived from the excess free energy of solution mixing. The Wilson equation for the ith component in a binary system (i,j) is described by equation 1.

$$\ln \gamma_i = -\ln(X_i + W_{ij}X_j) + X_j\left[\frac{W_{ij}}{X_i + W_{ij}X_j} - \frac{W_{ji}}{X_j + W_{ji}X_i}\right] \qquad (1)$$

X is the mole fraction in solution. The W_{ij} and W_{ji} are the Wilson coefficients. An advantage of this equation is that the general equation for three (i,j,k) or more components requires only the corresponding pairwise coefficients (i.e., $W_{ik}, W_{kj}, W_{ki}, W_{kj}$), eliminating the need for triplet coefficients.

Once the system Wilson coefficients are known, the vapor pressure, P_i, of the individual components are computed from the activity coefficients, γ_i, as shown in equation 2.

$$P_i = \gamma_i X_i P_i^{O} \qquad (2)$$

P_i° is the vapor pressure of the pure component at the solution temperature. The empirical Antoine equation provides the pure vapor pressures in equation 3.

$$\ln P_i^{O} = (\ln 10)\left(A_i - \frac{B_i}{t - C_i}\right) \qquad (3)$$

A_i, B_i, and C_i are the experimentally determined Antoine coefficients for the ith solution component, and t is the solution temperature in Celsius. For binary solutions, 1 represents the organic solute and 2 represents the solvent water.

The original literature data cited by Hirata et al. established the pairs of Wilson coefficients for the five binary systems. These data files range from as few as six references for water-MEK (50 data points) to as many as 22 references for water-ethanol (298 data points). The original vapor pressure data for each of these files are either isobaric or isothermal. Isobaric indicates that the vapor mole fraction and temperature are in equilibrium with the solution mole fraction at a specified constant total pressure. Isothermal refers to the condition of the vapor mole fraction and total pressure in equilibrium with the solution mole fraction at a specified constant temperature. Besides the binary solution vapor pressures, the vapor pressures of the pure components are also needed in computing the Wilson coefficients. Following the approach of Hirata et al., these coefficients are evaluated using two distinct sets of Antoine coefficients for all but the MEK component. Table 2 summarizes the sets of Antoine coefficients for the systems considered. There is not an apparent correlation or consistency in which Antoine coefficient set is applied by Hirata et al. for a given binary solution. In a few instances, selecting one or the alternate set of Antoine coefficients yields unrealistic (i.e., negative) Wilson coefficients that are unacceptable. The differences in the vapor pressures of the pure components predicted by each Antoine coefficient set are small and appear to furnish a better vapor pressure fit for either the high or low ends of the liquid temperature range. Rather than an arbitrary selection of Antoine coefficients, the present study recalculates the pairs of Wilson coefficients for each literature citation (data file), using all four combinations of Antoine coefficients (i.e., water-organic, W-O: 1-1, 1-2, 2-1, and 2-2). The pair of Wilson coefficients yielding the best fit is determined. The set of Antoine coefficients that resulted in the best fit Wilson coefficients are listed in the last two columns of Table 3. The criteria for best fit of the Wilson coefficients is the smallest average deviation of the vapor mole fraction given in equation 4.

$$\delta Y = \frac{1}{N}\sum_{i=1}^{N} |Y_i(calc) - Y_i(obs)| \qquad (4)$$

The average deviation for the temperature, δT, is similarly defined. These figures of merit are consistent with those used by Hirata et al. and allow an additional verification of the vapor pressure computations. The percent variation in the average deviation of the vapor mole fraction, $\%\delta Y$, for the water-methanol system (i.e., $100*\delta Y$) is tabulated in column 6 of

Table 3; whereas the average deviation for the temperature, δT, is listed in column 7.

The computation of the pair of Wilson coefficients for a given data file minimizes the residual sum of squares for the excess Gibbs free energy of solution:

$$SQ = \sum r_i^2, \tag{5}$$

where

$$r_i = \sum X_i \ln \gamma_i(obs) - \sum X_i \ln \gamma_i(calc), \tag{6}$$

with

$$\gamma_i(obs) = \left(\frac{Y_i}{X_i}\right)\left(\frac{P_T}{P_i^O}\right) \tag{7}$$

and ln γ_i(calc) is calculated from the Wilson equation (i.e., equation 1). Y_i is the vapor mole fraction and P_T is the total vapor pressure in equation 7. Substitution of equation 1 and equation 7 into equation 6 produces a non-linear expression for a two component system, namely equation 8:

$$r_i = \left[X_1 \ln\left(\frac{Y_1}{X_1}\right)(X_1 + W_{12}X_2) - X_1 \ln\left(\frac{P_i^O}{P_T}\right) + X_2 \ln\left(\frac{Y_2}{X_2}\right)(W_{21}X_1 + X_2) - X_2 \ln\left(\frac{P_2^O}{P_T}\right)\right]_i \tag{8}$$

The minimization of SQ is performed by setting $(\partial SQ/\partial W_{12})=0$ and $(\partial SQ/W_{21})=0$. This gives two difference equations in ΔW_{12} and ΔW_{21}.

$$\Delta W_{12} \sum D1_{i2} + \Delta W_{21} \sum (D1_i + D2_i) = \sum (D1_i r_i) \tag{9}$$

$$\Delta W_{12} \sum (D1_i + D2_i) + \Delta W_{21} \sum D2_{i2} = \sum (D2_i r_i) \tag{10}$$

where

$$D1_i = \left(\frac{X_1 X_2}{X_1 + W_{12} X_2} \right)_i \tag{11}$$

$$D2_i = \left(\frac{X_1 X_2}{X_{21} X_1 + X_2} \right)_i \tag{12}$$

Equations 9 and 10 that are defined by equations 11 and 12 are solved simultaneously for ΔW_{12} and ΔW_{21} by the proper selection of values for W_{12} and W_{21}. Initial values of 0.5 are selected for the Wilson coefficients. The computation of Wilson coefficients is subsequently iterated by setting $W_{ij}(new) = W_{ij}(old) - \Delta W_{ij}$. This iteration process continues until the differences are below a desired threshold value (e.g., $|\Delta W_{12}| + |\Delta W_{21}| < 10^{-5}$ to be consistent with Hirata's computational approach).

The calculation of the Wilson coefficients for all data files of a specific two component systems produces one pair of Wilson coefficients for each file. Hirata et al. have observed that variation of W_{12} with respect to W_{21} for a given data file results in a minimum in SQ that shifts with the value of W_{21}. Thus, a single minimum exists along this hyperbolic path. Although Hirata et al. do not address the selection of the best single Wilson coefficient pair to represent all the data files given for a two component system, this investigation demonstrates all the systems possess a similar single minimum for δY. The pair of Wilson coefficients for this minimum are close but not identical to the mean values calculated over the array of pairs computed from the data files. Table 3 shows these results in columns 4 and 5. The actual "best pair" of Wilson coefficients are found by a grid search spanning the entire array of pairs. Figure 2a presents a global $\%\delta Y$ error graph for W_{21} versus W_{21}, whereas Figure 2b is the projected two dimensional contour plot of the minimum $\%\delta Y$ errors derived from the grid search. The $\%\delta Y$ value that is designated by the dash lines in Figure 2b locates the minimum for the aqueous methanol system. The Wilson coefficient values at the minimum $\%\delta Y$ are given in Table 3 as the best values. Table 3 provides a summary of the computed results for the water-methanol system. Columns 8, 9, and 10 (Table 3) list the percentage for the individual, mean, and best estimate of the standard error in the vapor mole fraction, respectively. The Wilson coefficients for the water-methanol system are reported in the last two rows of Table 3, which are labeled MEAN and BEST. In calculation of the mean and best Wilson coefficients, the W_{12} coefficient associated with reference file number 523 is rejected as an outlier by the Grubb's test[12,13]

at the 99.5% confidence level. Thus, both Wilson coefficients for reference file number 523 must be rejected. Table 4 supplies a synopsis of the results for the five binary systems studied with the mean and best Wilson coefficient values.

The pair of Wilson coefficients established for each system allow calculation of the vapor pressures at 22 °C for the seven solutions of each binary system, based on the solution mole fractions with the exception of only four concentrations for the MEK-water system. The mole fractions of each solution are computed directly from the measured weights of the components. These weights have been determined to be within 0.01 g for total solution weights of around 170 g. Table 1 summarizes the compositions and vapor pressures that are used in accessing the adherence of the associated IR absorbances to Beer's Law.

Infrared interferograms are acquired with the equilibrium vapor cell for 32 aqueous solutions equilibrated at 22 °C. The solution compositions are listed in Table 1 by percent solute mole fraction in the solvent and the associated solute vapor pressure developed over the solution. The methanol vapor provides the opportunity to investigate the onset of rotational fine structure at 1 cm^{-1} spectral resolution for the P and R branches near 1014 and 1054 cm^{-1}, respectively. The PQR branch contour centered at 1033 cm^{-1} is devoid of other spectral features in the 800 to 1200 cm^{-1} region. Integration of the PQR absorbance band contour and use of the path averaged concentration permits a comparison of the absorbance measurements for this investigation to those of other laboratories. The absorbance measurements for methanol are made at 0.56, 1, 2, and 4 cm^{-1} spectral resolutions. These measurements allow an evaluation of the interferogram apodization effect on the absorbance measurements. The remaining solute absorbances are determined from interferograms with a 2 cm^{-1} spectral resolution. Select absorbance bands in the spectral region from 800 to 1400 cm^{-1} are used in calculation of the absorptivities. The absorptivities that are obtained with the EVC approach are compared to those of other investigators.

Methanol vapor pressures are varied from 5.7 to 37.9 torr, which corresponds to a path averaged concentration from 758 to 5039 ppm-m with a 10-cm pathlength cell. The corresponding water vapor pressures range from 19.1 to 15.4 torr with the path averaged concentrations ranging from 2540 to 2048 ppm-m. The methanol absorbances for a methanol vapor pressure are about 1000 times stronger than those of water at 2000 ppm-m in the 800 to 1200 cm^{-1} spectral region.[14] The blank cell serves to ratio out this contribution from the water vapor absorbances. The absorbance measurements for the PQR bands at 0.56 cm^{-1} spectral resolution, using a box car apodization, are plotted as a function of vapor pressure in Figure 3. The open symbols represent the least squares calculated absorbances and the solid

symbols denote the measured values. The P and R bands adhere well to Beer's Law with absorbance versus vapor pressure slopes of 0.03200 ± 0.00029 and 0.04034 ± 0.00022, respectively. On the other hand, the Q branch shows a marked deviation from Beer's Law with a slope of 0.0530 ± 0.0017. This deviation from Beer's Law occurs, because the spectrometer resolution of 0.56 cm^{-1} is inadequate to resolve the narrow Q band.

The Beer's Law slopes for the methanol P and R branches are shown as a function of spectral resolution and apodization in Table 5. The lower spectral resolutions are generated by the appropriate truncation of the 0.56 cm^{-1} resolution interferograms. The effect of apodization does not generally become pronounced until a spectral resolution of 1 cm^{-1} or greater is reached. This has also been confirmed for all other solute vapor spectra collected at 2 cm^{-1} spectral resolution in this study. At 1 cm^{-1} spectral resolution, the magnitude of absorbance versus vapor pressure slopes follow the expected trend in the apodized absorbance spectra of box car > medium Norton Beer > triangular.

The integrated absorbance area of a spectral band is independent of the spectrometer's line shape function.[15] Therefore, the absorbance areas permit a comparison of experimental results between spectrometers that are operated at different spectral resolutions. A comparison of methanol absorbance spectra from this investigation to those of three other laboratories is made with Figure 4.[14,16,17] Figure 4 shows a plot of PQR band absorbance area versus path averaged concentration (e.g., ppm-m). The limits of band integration are established by computing the best estimate of the standard deviation (BESD) over two 180 cm^{-1} intervals positioned on each side of the PQR band contour. The lower interval begins at 700 cm^{-1} and the upper starts at 1120 cm^{-1}. The BESDs for these intervals are calculated with successive differences as shown in equation 13.

$$BESD = \sqrt{\frac{\sum_{i=1}^{n-1} [A(\bar{\nu}_{i+1}) - A(\bar{\nu}_i)]^2}{2[n-1]}} \qquad (13)$$

The ν_i denotes a specified wavenumber, and $A(\nu_i)$ represents the absorbance at that specified wavenumber. The application of the successive difference method for calculation of the BESD for spectra is documented by Mark and Workman.[18] The first absorbance value approaching the PQR band that exceeds three times the calculated BESD is designated as an integration limit. Therefore, the integration limits are effectively defined in terms of the absorbance spectra noise. Integration of the PQR absorbance band is subsequently performed with the trapezoidal integration routine available in Spectra Calc. The integration results for

the methanol PQR band are shown in Figure 4. The integrated absorbances demonstrate reasonable agreement with the exception of the measurement in reference 16.

A comparison of absorbances, at the same spectral resolution, is required to compare the absorptivities at a particular wavenumber. The absorbance spectra from references 14, 17, and 16 possess resolutions of 0.125, 0.25, and 2 cm^{-1}, respectively. Therefore, the absorbance spectra for references 14 and 17 are adjusted to a 2 cm^{-1} resolution for purposes of comparison by introduction of fractional values, p (i.e., either 0.0625 or 0.125) into equation 14.

filter #s,0,1,p,1,p,0,1,0 (14)

The expression given in equation 14 is the Spectra Calc Fourier filtering function that reduces the spectral resolution of the absorbance source spectrum by 1/p.

The absorbance spectra at 2 cm^{-1} resolution are used in calculation of the absorptivities. If only a single measurement is available, then Beer's Law is solved algebraically for the absorptivity, α. When three or more measurements are available, the absorptivity is calculated from the least squares slope of absorbance versus concentration. The gas concentration in grams per cubic meter is determined from the vapor pressure in torr by the ideal gas law that is shown in equation 15.

$$C\left(\frac{g}{m^3}\right) = \frac{16.034 M P_{vap}}{T} \qquad (15)$$

T is the vapor temperature in degrees Kelvin; M is the molecular weight of the vapor solute in grams/mole; P_{vap} is the vapor pressure in torr; and 16.034 is the reciprocal of the ideal gas law constant in units of mole Kelvin/cubic meter torr (mol·K)/(m^3·torr). The final units for the absorptivity are square meters/milligram (m^2/mg). The absorptivities, α, are calculated for a 2 cm^{-1} spectral resolution and are summarized for all solute vapors studied in Table 6.

The resultant absorptivities in Table 6 show significant variation between the laboratories. The experimental precision in the EVC measurements for the bands selected in Table 6 is as follows: Methanol/P, ±0.8%, /Q, ±4%, and /R, ±0.5%; Ethanol/ ±2%; Isopropanol/ ±2%; Acetone/ ±0.5%; and MEK/ ±2%. Only the 1072 cm^{-1} band of isopropanol for reference 14 falls within the EVC experimental precision. The remaining isopropanol absorptivities for reference 14 are within about 7% of the EVC

results. The methanol absorptivities for reference 17 are within 9% of the EVC findings for the P and R bands. The methanol P and R band absorptivity results for reference 14 differ about 20% from those of the EVC. The remaining absorptivities in Table 6 vary from the EVC evaluations by 30 to 70%. This clearly indicates a need for accurate and critically evaluated vapor phase absorbance measurements.

The EVC method provides a solute vapor pressure accurate to within 2%. The EVC absorbance versus vapor pressure measurements provide slopes with a precision of ±2% or better. These slopes are measured over the Beer's Law range for a statistically significant number of concentrations. In the case of acetone only four vapor concentrations show adherence to Beer's Law for the intense 1217 and 1365 cm^{-1} bands. This is shown with the absorbance versus vapor pressure plot in Figure 5 for the bands of Table 6. An added benefit of the EVC method is the controlled presence of water vapor. This permits the assessment of the absorptivities for conditions similar to those found in many open-path FTIR spectrometry applications.

4. CONCLUSIONS

Quantitative measurement of vapors in the atmosphere with open-path Fourier transform infrared (FTIR) spectrometry demands the use of accurate absorptivities. A comparison of interlaboratory absorptivities exhibits significant variation. The integration of the methanol PQR absorbance band furnishes a criterion for correlating absorbance measurements from different laboratories.

The present study advocates the use of aqueous solutions for generation of selected solute vapors at specific concentrations with a 2% accuracy. Analysis of the available literature vapor pressure data permits an assessment of the best Wilson coefficients for each binary system studied. The resultant best coefficient values along with the vapor pressures of the pure solution components allow an accurate evaluation of the solute and the solvent vapor concentrations for equilibrium conditions. An air/vapor mixture is continuously closed looped circulated through the fixed temperature aqueous solution and infrared (IR) flow cell to insure solution equilibrium. A statistically significant number of vapor concentrations establishes the linear region of IR absorbance measurements (i.e., Beer's Law). The resultant experimental precision for the absorptivities is ±2% or better for the systems studied.

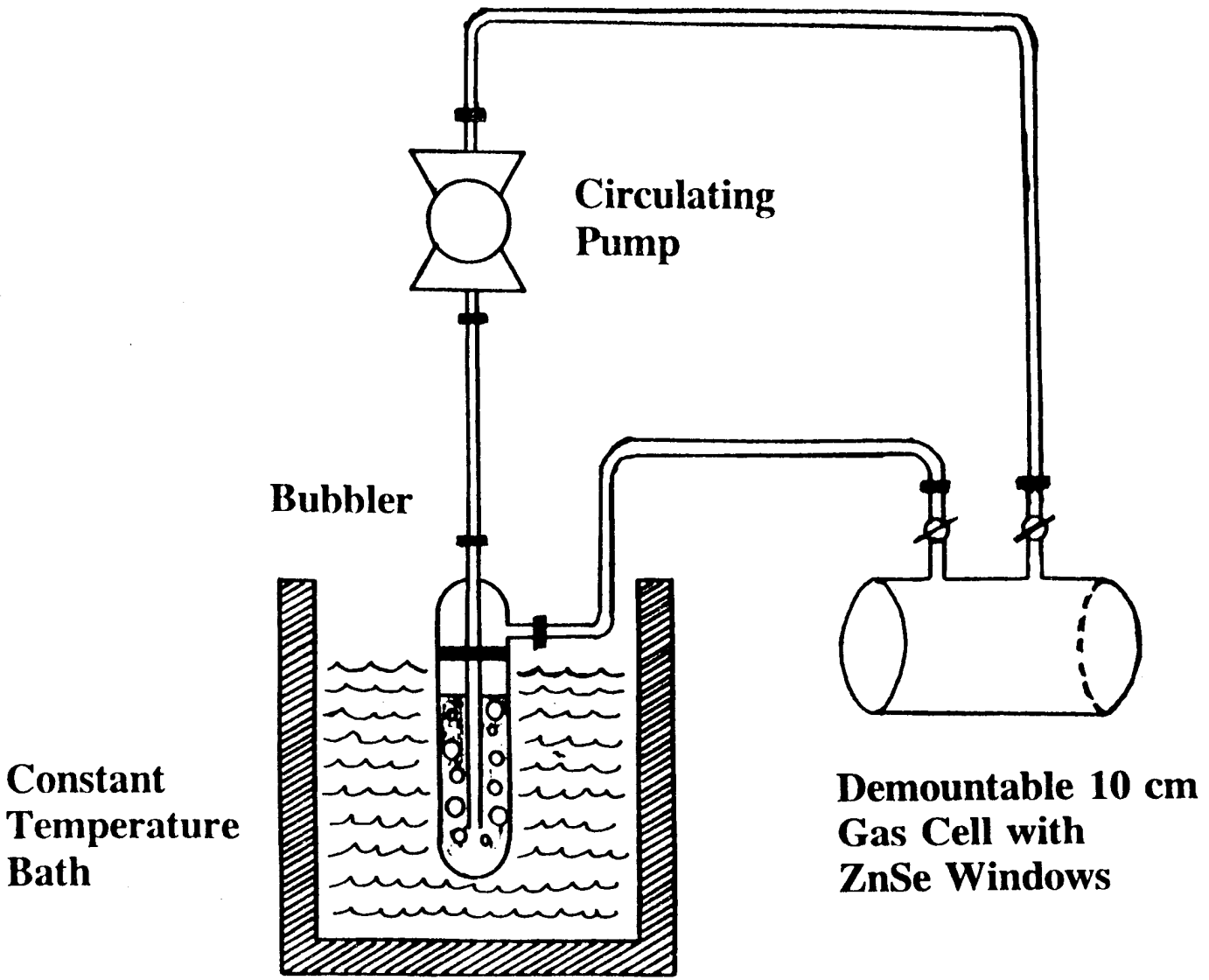

Figure 1. Equilibrium Vapor Cell

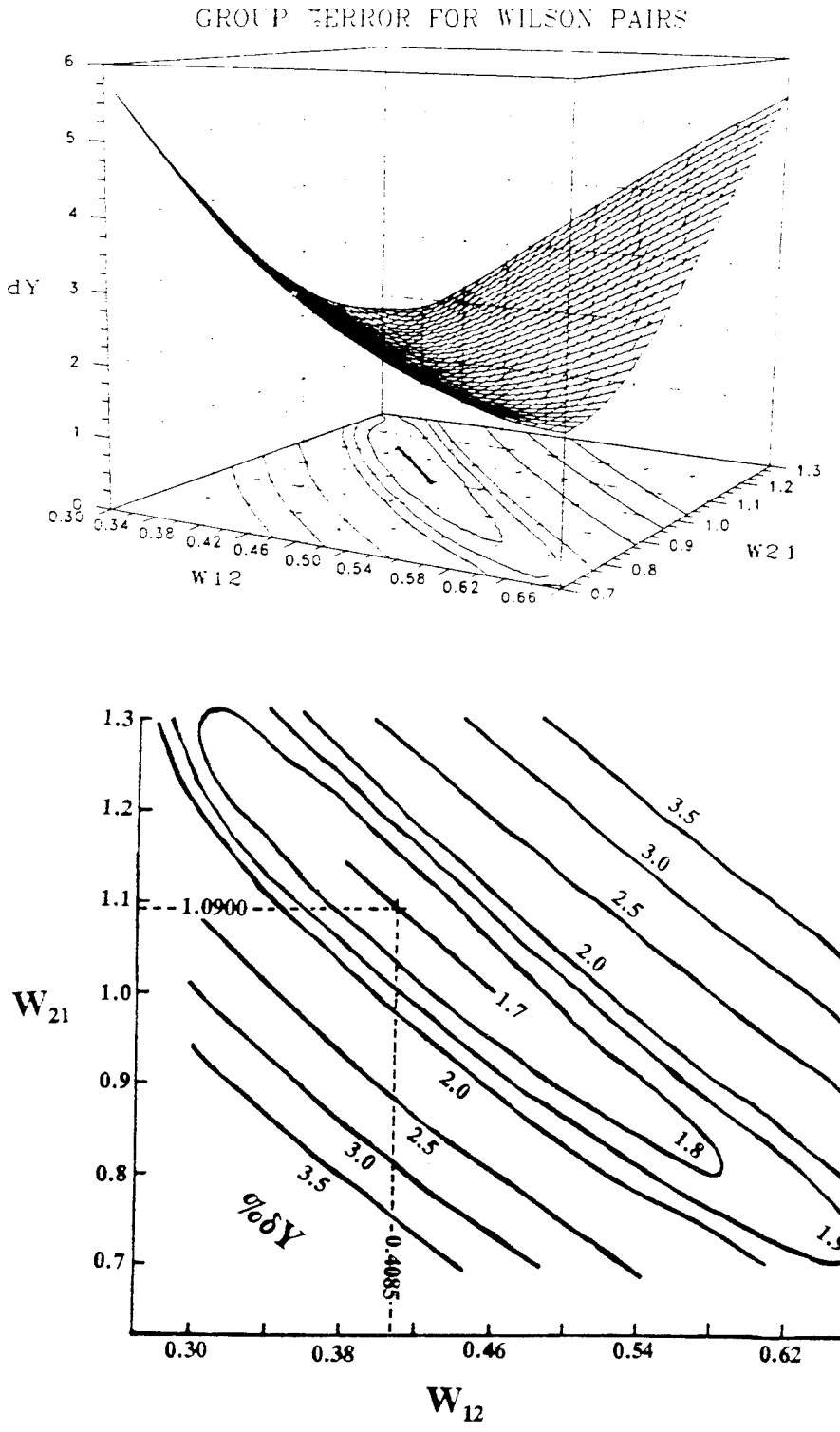

Figure 2. Wilson Coefficient Error Graphs: (A) Global Three Dimensional Percent Error Surface and (B) Two Dimensional Projected Contour Percent Error Plot

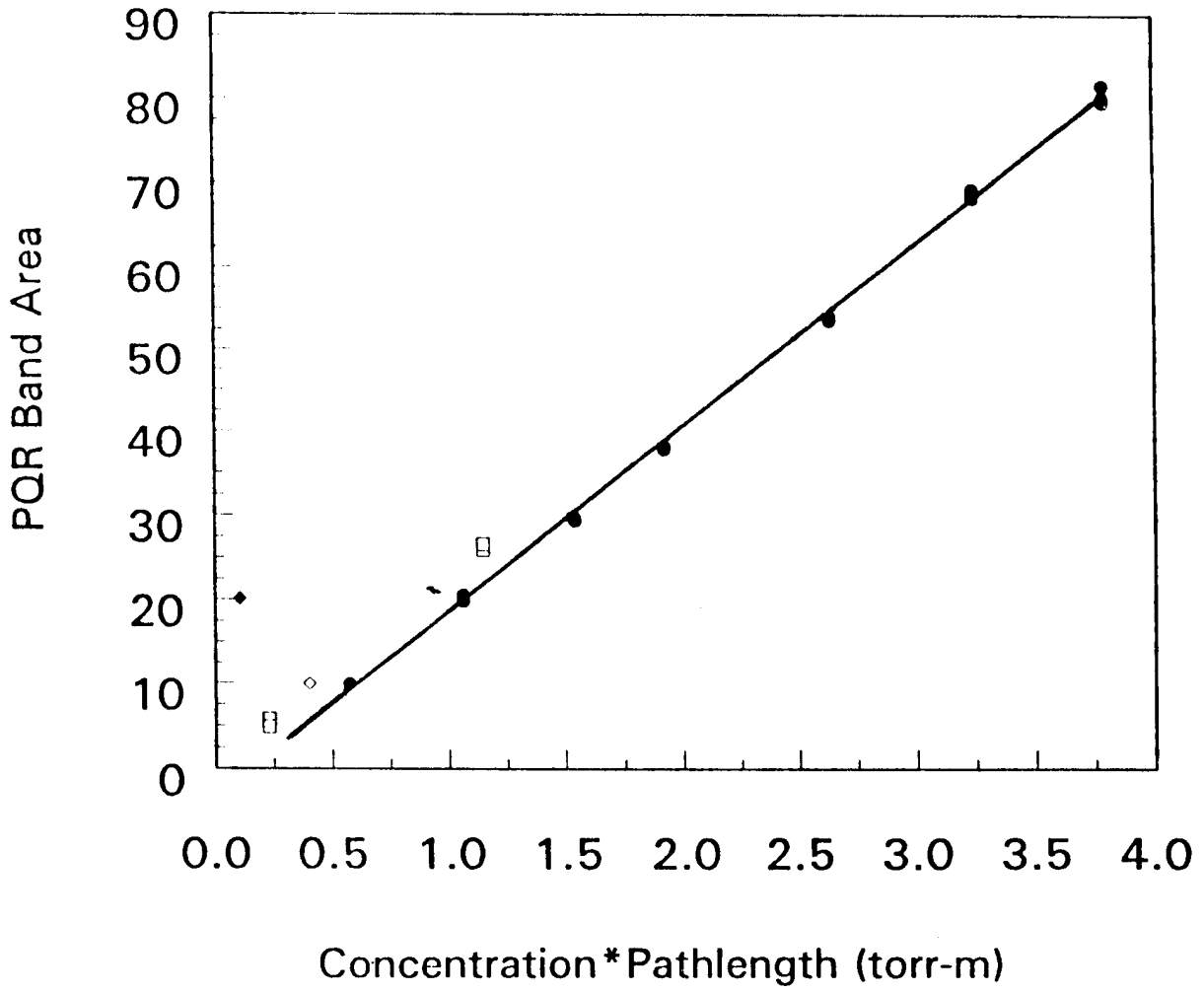

Figure 3. Comparison of Methanol Absorbances

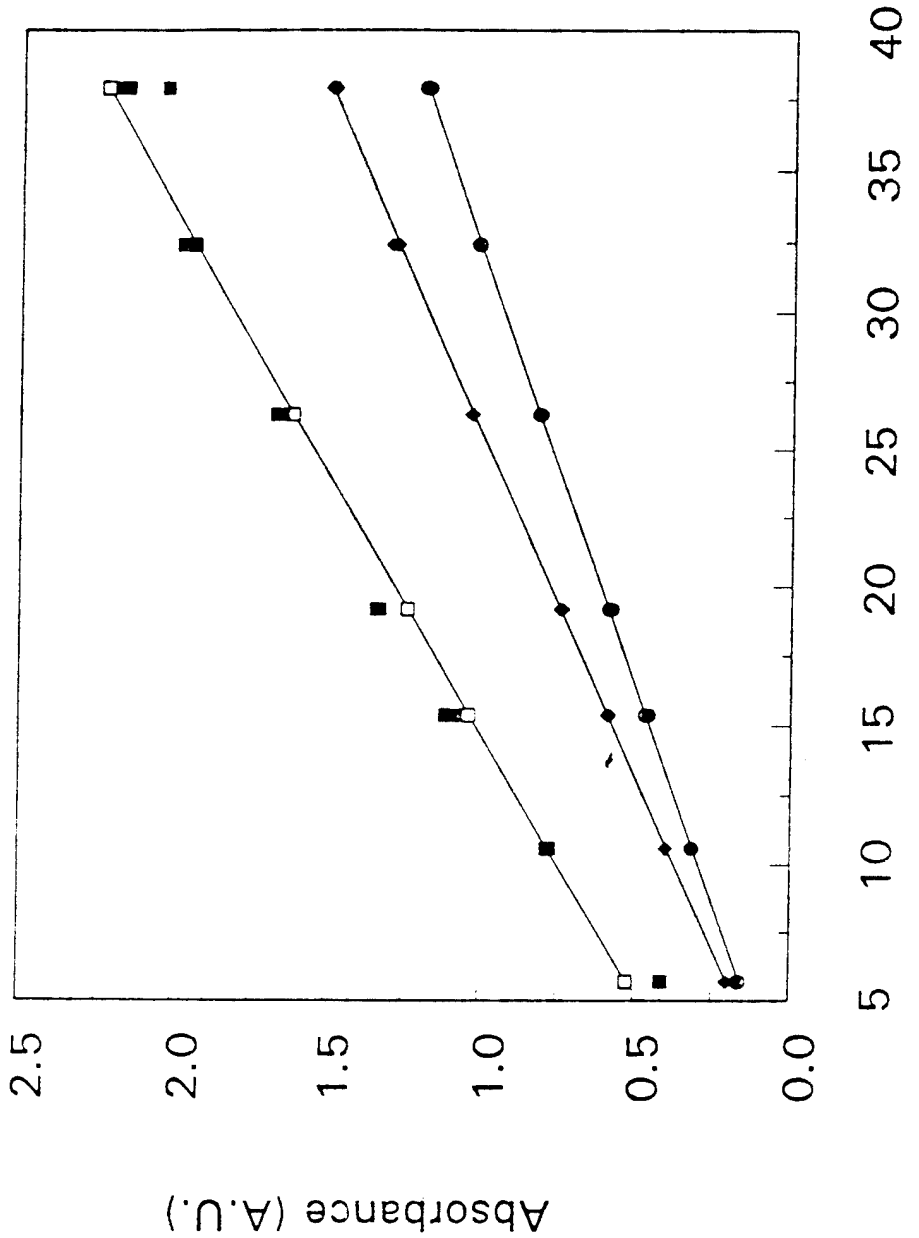

Figure 4. Methanol Absorbances at 0.5 cm

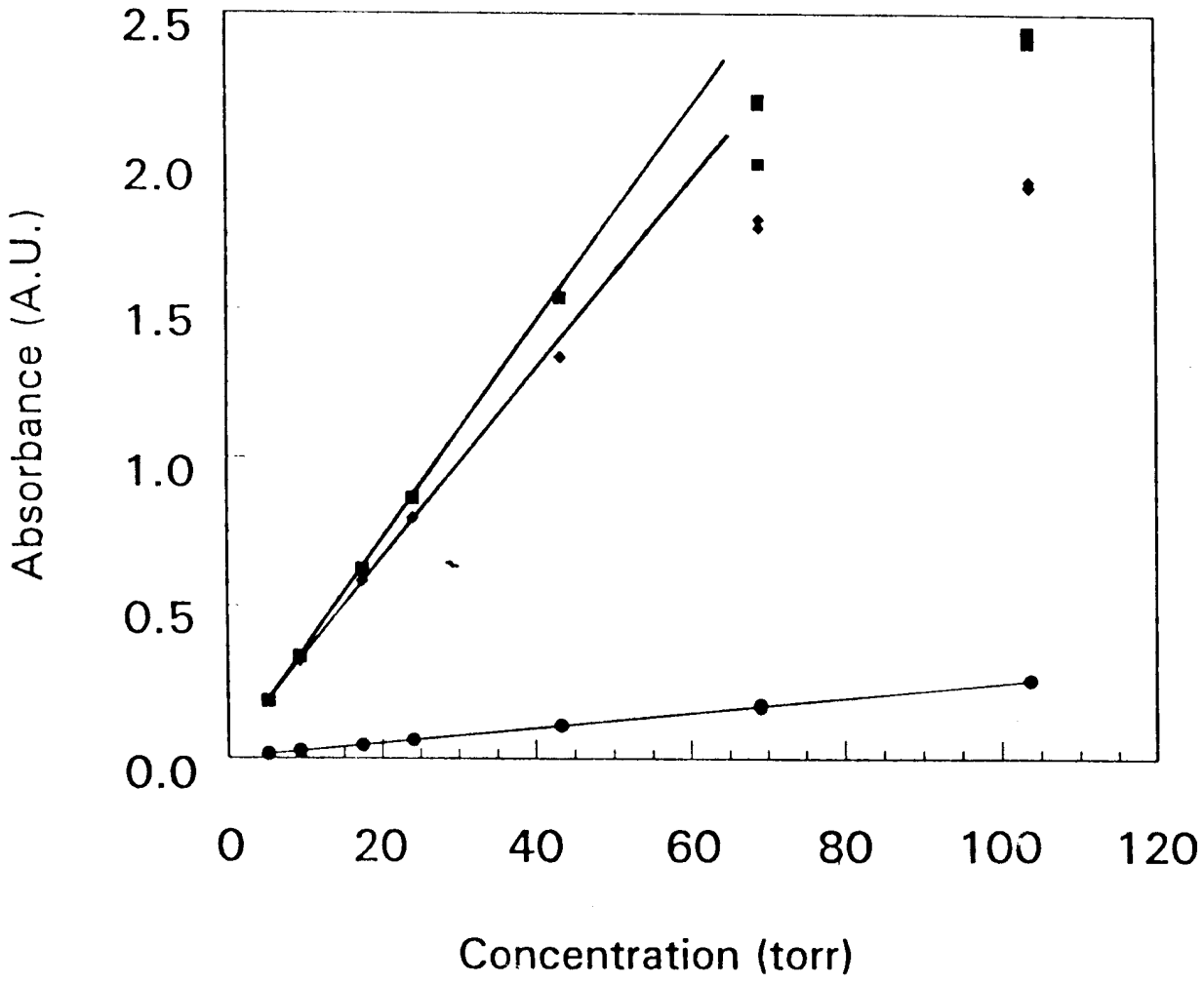

Figure 5. Acetone Absorbance at 2 cm

Table 1. Solute Mole Percent and Associated Vapor Pressures at 22 °C

Methanol		Ethanol		Isopropanol		Acetone		Methyl Ethyl Ketone	
MOL. (%)	P_{vap} (torr)	MOL. (%)	P_{vap} (torr)	MOL. (%)	P_{vap} (torr)	MOL. (%)	P_{vap} (torr)	MOL. (%)	P_{vap} (torr)
2.52	5.7	2.02	4.7	1.91	5.1	0.29	5.2	0.65	27.7
4.98	10.6	5.08	9.7	6.01	9.8	0.53	9.3	1.31	40.1
7.66	15.4	10.02	14.7	30.01	15.1	1.05	17.5	2.61	50.2
10.00	19.2	25.03	22.3	55.00	17.8	1.50	24.1	5.00	56.0
15.00	26.3	40.11	27.1	70.02	19.9	3.09	43.3		
20.00	32.4	55.01	31.6	84.96	22.4	6.19	69.0		
24.97	37.9	64.96	34.8	100.00	25.9	15.0	103.7		

Table 2. Antoine Coefficients for Pure Solution Components

COMPONENT	COEFFICIENTS		
	A	B	C
Water,1	7.96681	1668.210	228.000
Water,2	8.10765	1750.286	235.000
Acetone,1	7.02447	1162.000	224.000
Acetone,2	7.23967	1279.870	237.500
MEK(1)	6.97421	1209.600	216.000
Methanol,1	7.87863	1473.110	230.000
Methanol,2	8.07246	1574.990	238.960
Ethanol,1	8.04494	1554.300	222.650
Ethanol,2	8.16290	1623.220	228.980
Isopropanol,1	6.66040	813.055	132.930
Isopropanol,2	7.75634	1356.142	197.970

Table 3. Determining of Best Wilson Coefficients for Methanol-Water System

REF	P_{vap} (torr)	T (°C)	# pts.	W_{12}	W_{21}	%δY	%δT	$\%S_{Y_i}$	$\%S_{Y_m}$	$\%S_{Y_b}$	W	O
513	735	66-97	8	0.4069	0.7956	1.69	0.78	1.93	5.47	5.15	2	2
514	760	71-93	16	1.4842	0.1513	4.01	1.40	4.83	3.53	3.24	1	2
515	760	65-96	15	0.4182	1.0010	0.84	0.23	0.97	0.64	0.48	2	1
516	760	66-96	21	0.4753	0.9836	0.93	0.40	1.22	1.39	1.10	1	2
517	760	65-96	14	0.4616	0.9516	1.19	0.43	1.53	1.04	1.02	1	1
518	760	64-100	26	0.7782	0.6153	2.11	0.38	2.84	2.25	2.04	1	1
519	2280	96-134	22	0.3118	0.9866	2.39	1.00	3.30	1.11	1.05	1	2
520	3800	112-148	22	0.1136	1.4664	2.71	1.21	4.90	1.62	1.71	1	1
521	6080	129-167	22	0.4621	0.8473	2.06	0.90	2.49	1.08	1.08	2	2
522	8512	143-182	22	0.2073	1.3306	2.96	1.15	3.74	2.55	2.65	1	1
523	68-245	40	21	2.4319*	0.0851.	6.90*	0.04*	8.60	3.72	3.66	1	2
524	119-391	50	12	0.2842	1.6579	2.08	0.02	3.05	2.19	2.38	2	1
525	183-539	60	12	0.4505	1.0747	0.79	0.01	0.92	0.91	1.09	2	1
526	780-2529	100	12	0.2333	1.4452	1.17	0.01	1.74	1.22	1.30	2	2
527	3822-7940	140	6	0.4359	1.0598	1.00	0.06	1.07	1.01	1.13	1	1
528	3790-10298	150	11	0.1709	1.3959	2.94	0.03	3.87	2.52	2.51	1	1
529	12205-29580	200	11	0.1393	1.5701	4.09	0.05	4.95	3.79	3.94	1	1
		Mean:		0.4271	1.0833	2.34	0.47	3.06	2.12	2.09		
		Best:		0.4085	1.0900	1.685						

Table 4. Mean and Best Wilson Coefficient Values

System	Mean		Best	
	W_{12}	W_{21}	W_{12}	W_{21}
Water-Methanol	0.4271	1.0833	0.4085	1.0900
Water-Ethanol	0.1395	1.0260	0.1950	0.9104
Water-Isopropanol	0.0693	0.7431	0.0989	0.6597
Water-Acetone	0.1814	0.4896	0.1768	0.5148
Water-MEK	0.0835	0.3415	0.0242	0.2721

Table 5. The Effect of Apodization on Least Squares Slopes for the Methanol Vapor P and R Branches at Various Resolutions. All slope values are scaled by 10^2.

ν (cm^{-1})	$\Delta\nu$ (cm^{-1})	APODIZATION		
		Boxcar	Medium Norton-Beer	Triangular
1015.1	4	2.550±0.016	2.551±0.015	2.543±0.016
1014.8	2	2.712±0.021	2.578±0.016	2.552±0.016
1013.7	1	3.260±0.025	2.887±0.018	2.826±0.018
1013.7	0.56	3.200±0.019	3.054±0.018	2.950±0.017
1057.6	4	3.751±0.029	3.777±0.029	3.861±0.037
1057.3	2	3.742±0.027	3.930±0.029	3.836±0.037
1055.2	1	3.914±0.021	3.851±0.050	3.814±0.023
1057.6	0.56	3.963±0.033	3.939±0.032	3.920±0.032

Table 6. Comparison of Absorptivities at 2 cm^{-1} Spectral Resolution

Methanol		Ethanol		Isopropanol		Acetone		Methyl Ethyl Ketone	
ν (cm^{-1})	$\alpha*10^4$	ν (cm^{-1})	$\alpha*10^4$	ν (cm^{-1})	$\alpha*10^4$	ν (cm^{-1})	$\alpha*10^4$	ν (cm^{-1})	$\alpha*10^4$
1013.7	1.70[a]	879.80.26[b]		957.00.84[b]		1091.70.10[a]		940.10.12[a]	
1014.8	1.55[b]	879.50.47[c]		957.61.32[c]		1092.10.08[b]		941.50.06[b]	
1013.7	2.60[c]	879.30.53[d]		957.00.81[d]		1091.70.11[c]		940.10.20[c]	
1013.7	1.94[d]					1091.80.12[d]			
		1028.30.74[b]		1072.80.62[b]				1175.00.62[a]	
1033.2	7.11[a]	1028.01.52[c]		1072.41.03[c]		1217.71.44[a]		1175.00.33[b]	
1034.1	2.50[b]	1027.71.38[d]		1072.80.61[d]		1217.51.12[b]		1175.11.03[d]	
1032.8	7.44[c]					1217.01.81[c]			
1033.3	8.00[d]	1066.91.38[b]		1151.90.85[b]		1217.21.89[d]		1367.50.58[a]	
		1066.62.90[c]		1151.51.42[c]				1366.00.31[b]	
1053.5	2.23[a]	1066.22.41[d]		1150.80.81[d]		1365.41.47[a]		1367.50.97[c]	
1053.8	2.15[b]					1366.00.94[b]			
1053.1	3.82[c]	1242.50.32[b]		1252.2.58[b]		1365.51.64[c]			
1053.4	2.61[d]	1241.10.78[c]		1251.7.92[c]		1365.41.95[d]			
		1241.20.78[d]		1251.5.54[d]					

Note: a, reference 17; b, EVC; c, reference 16; and d, reference 14.

LITERATURE CITED

1. R. M. Hammaker, W. G. Fateley, C. T. Chaffin, T. C. Marshall, M. D. Tucker, V. D. Makepeace, and J. M. Poholarz, "FTIR Remote Sensing of Industrial Atmospheres for Spatial Characterization," Applied Spectroscopy Vol. 47(9), pp 1471-1475 (1993).

2. M. L. Spartz, J. S. Eldridge, G. D. Hipple, W. K. Reagen, and J. W. Stock, "Industrial Applications of Open-path Fourier Transform Infrared Spectroscopy," in SPIE Proceedings of the 9th International Conference on Fourier Transform Spectroscopy, ed. J. E. Bertie and H. Wieser, Vol. 2089, pp 462-463, Society of Photo-Optical Instrumentation Engineers, Bellinghan, WA, 1993.

3. R. T. Kroutil, R. J. Combs, R. B. Knapp, and G. W. Small, "Automated Detection of Acetone, Methyl Ethyl Ketone, and Sulfur Hexafluoride by Direct Analysis of Fourier Transform Infrared Interferograms," Applied Spectroscopy Vol. 48(6), pp 724-732 (1994).

4. A. S. Bangalore, G. W. Small, R. J. Combs, R. B. Knapp, and R. T. Kroutil, "Automated Detection of Methanol Vapor by Open-path Fourier Transform Infrared Spectrometry," Analytica Chimica Acta Vol. 297, pp 387-403 (1994).

5. S. L. Monfre and S. D. Brown, "Quantitative Fourier-Domain Analysis. Part I: Analysis of Raw FTIR Interferograms," Applied Spectroscopy Vol. 46(11), pp 1699-1710 (1992).

6. H. Xiao and S. P. Levine, "Application of Computerized Differentiation Technique to Remote-Sensing Fourier Transform Infrared Spectrometry for Analysis of Toxic Vapors," Analytical Chemistry Vol. 65(17), pp 2262-2269 (1993).

7. P. L. Hanst, "Air Pollution Measurement by Fourier Transform Spectroscopy," Applied Optics Vol. 17(9), pp 1360-1366 (1978).

8. G. O. Nelson, Gas Mixtures Preparation and Control, Lewis Publishers, London, England, 1992.

9. G. M. Wilson, "Vapor Liquid Equilibrium. XI A New Expression for Excess Free Energy of Mixing," Journal of the American Chemical Society Vol. 86(2), pp 127-130 (1964).

10. M. Hirata, S. Ohe, and K. Nagahama, Computer Aided Data Book of Vapor-Liquid Equilibria, Elsevier Scientific Publishing Company, Tokyo, Japan, 1975.

11. D. Kuehl, "An Optimized Programming Language/ Environment for Processing Scientific Data," Spectroscopy Vol. 4(1), pp 30-34 (1989).

12. John Keenan Taylor, Statistical Techniques for Data Analysis, pp 87-103, Lewis Publishers, Incorporated, CRC Press, Boca Raton, FL, 1990.

13. F. James Rohlf and Robert R. Sokal, Statistical Tables, 2nd ed., pp 213-124, W.H. Freeman and Company, San Franciso, CA, 1981.

14. Infrared Spectra for Quantitative Analysis of Gases, QASpec Spectra Library Lab-Calc Version, Infrared Analysis Incorporated, Anaheim, CA, 1992.

15. J. Park, "Effect of Interferogram Smearing on Atmospheric Limb Sounding by Fourier Transform Spectroscopy," Applied Optics Vol. 21(8), pp 1356-1366 (1982).

16. Quantitative Spectral Database, Interact Version 1.1, Sprouse Scientific Incorporated, Paolia, PA, 1991.

17. Quantitative Infrared Vapor Phase Spectra, EMTIC Extractive Technologies FTIR Spectral Data Base, U.S. Environmental Protection Agency, Research Triangle Park, NC, 1992.

18. H. Mark and J. Workman, Statistics in Spectroscopy, pp 61-67, Academic Press Incorporated, Boston, MA, 1991.